Density Functional Study of Neutral Salicylaldiminato Nickel(II) Complexes as Olefin Polymerization Catalysts

Mary S. W. Chan, Liqun Deng, and Tom Ziegler*

Department of Chemistry, University of Calgary, Calgary, Alberta, Canada T2N 1N4

Received January 24, 2000

The recent discovery of the ability of salicylaldiminato Ni(II) complexes to promote ethylene polymerization creates a potential for a new class of olefin polymerization catalysts. The major advantage of this type of catalyst is that they produce a neutral active center and thereby avoid the ion-pairing problems encountered with the homogeneous single-site catalysts in current use. The present DFT study investigates the polymerization mechanism of these neutral complexes as well as the electronic and steric effects of various substituents on the catalyst backbone. The addition of electron-withdrawing or -releasing substituents on the 5 position of the salicylaldiminato ring was found to result in small changes in the energies of the reactions in the polymerization mechanism. This is most likely due to the substituents' remoteness from the active center. Changing the electronic nature of the donor atoms resulted in larger shifts in energy. Finally, bulky substituents such as 2,6-diisopropylphenyl and 9-anthracenyl groups were found to have the largest effect on the reaction barriers and enthalpies in a direction that should substantially increase catalyst activity.

I. Introduction

The past decade saw a large increase of research activity in the area of single-site olefin polymerization catalysts. The art of catalyst design requires synthetic skills as well as an understanding of the factors that influence the fundamental steps of the polymerization process. The majority of the investigations reported up until now have focused on metallocenes (and related compounds) of early transition metals[1] or late transition metals with diimide ligands.[2] The polymerization mechanisms and the influence of the ligands on the activity of these catalysts are well established by experimental and theoretical investigations.

Transitional metal complexes possessing bidentate salicylaldimine ligands have been characterized for quite some time.[3] However, it was not until the past few years that they have been considered as olefin polymerization catalysts.[4] Recently, Grubbs' group demonstrated that some neutral salicylaldiminato nickel(II) complexes, whose skeleton structure appears in Figure 1, show catalytic activities rivaling those of metallocenes and diimide complexes.[5] This potentially opens the door to a new class of catalysts, as the active sites derived from these nickel complexes are neutral, thus reducing the ion-pairing problems encountered in the current catalysts.[6]

Preliminary experimental results indicate that substituents on the salicylaldiminato ring have dramatic effects on the catalyst activity. In particular, bulky substituents in the 3 position enhance the activity of the catalyst by approximately a factor of 3. An electron-releasing group (OMe) in the 5 position reduces the activity by a factor of 2, while an electron-withdrawing group (NO_2) enhances it by a factor of 10. Selected substituents investigated by Grubbs' group are summarized in Table 1 along with their observed activities. In addition, an induction period lasting from 5 to 20 min was observed for the systems without the bulky substituent at the 3 position. The most active NO_2-substituted system required the longest induction time. The cause of this induction period was postulated to be

(1) (a) Bochmann, M. *J. Chem. Soc., Dalton Trans.* **1996**, 255. (b) Ewart, S. W.; Sarsfield, M. J.; Jeremic, D.; Tremblay, T. L.; Williams, E. F.; Baird, M. C. *Organometallics* **1998**, *17*, 1502. (c) Richardson, D. E.; Alameddin, N. G.; Ryan, M. F.; Hayes, T.; Eyler, J. R.; Siedle, A. R. *J. Am. Chem. Soc.* **1996**, *118*, 11244. (d) Yamaguchi, Y.; Suzuki, N.; Mise, T.; Wakatsuki, Y. *Organometallics* **1999**, *18*, 996. (e) Woo, T. K.; Margl, P. M.; Lohrenz, J. C. W.; Blöchl, P. E.; Ziegler, T. *J. Am. Chem. Soc.* **1996**, *118*, 13021. (f) Margl, P. M.; Lohrenz, J. C. W.; Ziegler, T.; Blöchl, P. E. J. *Am. Chem. Soc.* **1996**, *118*, 4434.

(2) (a) Musaev, D. G.; Morokuma, K. *Top. Catal.* **1999**, *7*, 107. (b) Schleis, T.; Spaniol, T. P.; Okuda, J.; Heinemann, J.; Mülhaupt, R. *J. Organomet. Chem.* **1998**, *569*, 159. (c) Froese, R. D. J.; Musaev, D. G.; Morokuma, K. *J. Am. Chem. Soc.* **1998**, *120*, 1581. (d) Musaev, D. G.; Froese, R. D. J.; Morokuma, K. *Organometallics* **1998**, *17*, 1850. (e) Deng, L.; Woo, T. K.; Cavallo, L.; Margle, P. M.; Ziegler, T. *J. Am. Chem. Soc.* **1997**, *119*, 6177. (f) Deng, L.; Margl, P. M.; Ziegler, T. *J. Am. Chem. Soc.* **1997**, *119*, 1094. (g) Johnson, L. K.; Mecking, S.; Brookhart, M. *J. Am. Chem. Soc.* **1996**, *118*, 267. (h) Johnson, L. K.; Killian, C. M.; Brookhart, M. *J. Am. Chem. Soc.* **1995**, *117*, 6414. (i) Musaev, D. G.; Froese, R. D. J.; Svensson, M.; Morokuma, K. *J. Am. Chem. Soc.* **1997**, *119*, 367.

(3) (a) Holm, R. H.; Everett, G. W., Jr. *Prog. Inorg. Chem.* **1996**, *7*, 83. (b) Cozzi, P. G.; Callo, E.; Floriani, C. *Organometallics* **1995**, *14*, 4994. (c) Hunter, L.; Marriott, J. A. *J. Chem. Soc.* **1937**, 2000.

(4) (a) Matsui, S.; Tohi, Y.; Mitani, M.; Saito, J.; Makio, H.; Tanaka, H.; Nitabaru, M.; Nakano, T.; Fujita, T. *Chem. Lett.* **1999**, 1065. (b) Cameron, P. A.; Gibson, V. C.; Redshaw, C.; Segal, J. A.; Bruce, M. D.; White, A. J. P.; Villiams, D. J. *Chem. Commun.* **1999**, 1883. (c) Gibson, V. C.; Newton, C.; Redshaw, C.; Solon, G. A.; White, A. J. P.; Williams, D. J. *J. Chem. Soc., Dalton Trans.* **1999**, 827. (d) Corden, J. P.; Errington, W.; Moore, P.; Wallbridge, M. G. H. *Chem. Commun.* **1999**, 323.

(5) Wang, C.; Friedrish, S.; Younkin, T. R.; Li, R. T.; Grubbs, R. H.; Bansleben, D. A.; Day, M. W. *Organometallics* **1998**, *17*, 3149.

(6) (a) Chan, M. S. W.; Vanka, K.; Pry, C. C.; Ziegler, T. *Organometallics* **1999**, *18*, 4624. (b) Lanza, G.; Fragalá, I. L.; Marks, T. J. *J. Am. Chem. Soc.* **1998**, *120*, 8257. (c) Deck, P. A.; Beswick, C. L.; Marks, T. J. *J. Am. Chem. Soc.* **1998**, *120*, 1772. (d) Fusco, R.; Lango, L.; Proto, A.; Masi, F.; Garbassi, F. *Marcomol. Rapid Commun.* **1998**, *19*, 257.

10.1021/om000055+ CCC: $19.00
Publication on Web 06/14/2000

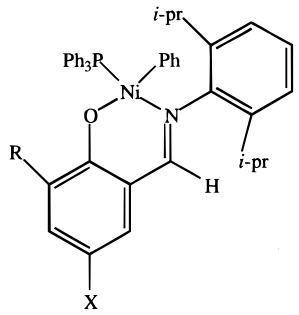

Figure 1. Skeleton structure of the salicylaldiminato nickel(II) complex.

Table 1. Experimental Substituents Effect on Catalyst Activity

R	X	activity (kg of PE/mol of Ni)
H	H	26.7
tert-butyl	H	46.7
Ph	H	81.3
9-phenanthrenyl	H	93.3
9-anthracenyl	H	98.7
H	OMe	13.3
H	NO_2	253.3

the slow abstraction of the phosphine group from the nickel, but very little is known regarding the polymerization mechanism of these systems. The purpose of the present study is to investigate the polymerization mechanism evoked by these salicylaldiminato complexes in order to explain the above experimental observations and to understand how substituents on the salicylaldiminato rings influence the activity of the catalyst and the length of the induction period.

The structure of the catalysts selected for the present density functional investigation is shown in Figure 2. The growing polymer is modeled by a propyl chain in all cases. The electronic effect of substitution at the 5 position of the salicylaldiminato ring is studied by a model system where the 2,6-diisopropylphenyl group and the bulky aryl group on the 3 position are replaced with hydrogen atoms. The reference system **1** does not have any substitution, while an electron-donating methoxy group is introduced in **2** and an electron-withdrawing nitro group system **3**. System **4** probes the influence of the 2,6-diisopropylphenyl group, while system **5** investigates the effect of the bulky 9-anthracenyl group. Finally, the effect of replacing the donor atom with phosphorus instead of nitrogen was examined in system **6**. Systems **4**, **5**, and **6** contain too many atoms for full quantum calculations to be feasible. These systems were studied using a combined quantum mechanics/molecular mechanics (QM/MM) approach,[7] where the 2,6-diisopropylphenyl and 9-anthracenyl groups are treated as molecular mechanics potentials. Details of the partitions are given in the Computational Details section.

The fundamental steps of the polymerization process include the generation of the active catalyst, chain propagation, and termination. Scheme 1 shows a pictorial representation of each of these elementary reactions using the model system **1**. The generation of the active site initiates the polymerization process. For the salicylaldiminato complexes studied by Grubbs, this required the removal of a phosphine ligand. This activation process was modeled by the dissociation reaction depicted by reaction 1 in Scheme 1. Chain propagation begins by the capture of a monomer molecule by this activated catalyst followed by insertion into the nickel–carbon bond. This series of steps is represented by reaction 2. One mechanism for termination is β-hydrogen transfer (BHT), where one of the hydrogen atoms on the β carbon is transferred a monomer attached to the metal coordination sphere, as illustrated by reaction 3 in Scheme 1. An alternative mechanism of termination is β-hydrogen elimination (BHE) (reaction 4, Scheme 1), where the hydrogen atom is transferred to the metal to produce a metal hydride. Previous theoretical studies have demonstrated that β-hydrogen transfer is the preferred pathway for both the metallocene type[8] and the diimine type catalysts.[2d,e] However, this may not be true for the salicylaldiminato systems, and therefore, both termination pathways will be investigated.

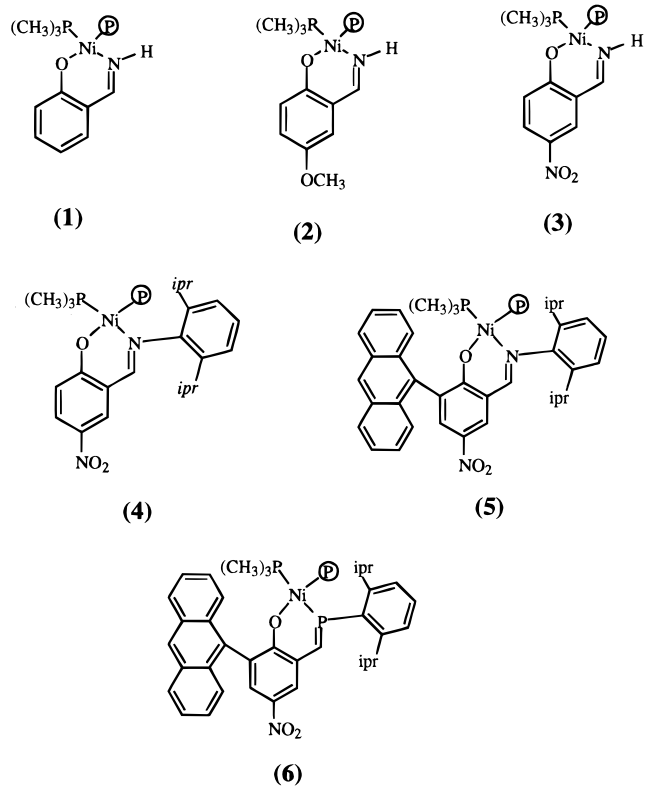

Figure 2. Structures of nickel complexes studied.

II. Computational Details

Stationary points on the potential energy surface were calculated with the Amsterdam Density Functional (ADF) program (version 2.3.3) developed by Baerends et al.[9] and vectorized by Ravenek.[10] The numerical integration scheme applied for the calculations was developed by te Velde et al.[11] The geometry optimization procedure was based on the method

(7) (a) Maseras, F.; Morokuma, K. *J. Comput. Chem.* **1995**, *16*, 1170. (b) Singh, U. C.; Kollman, P. A. *J. Comput. Chem.* **1986**, *7*, 718. (c) Field, M. J.; Bash, P. A.; Karplus, M. *J. Comput. Chem.* **1990**, *11*, 700.

(8) Lohrenz, J. C. W.; Woo, T. K.; Fan, L.; Ziegler, T. *J. Organomet. Chem.* **1995**, *497*, 91.

(9) (a) Baerends, E. J.; Ellis, D. E.; Ros, P. *Chem. Phys.* **1973**, *2*, 41. (b) Baerends, E. J.; Pos, P. *Chem. Phys.* **1973**, *2*, 52.

(10) Ravenek, W. *Algorithms and Applications on Vector and Parallel Computers*; te Riele, H. J. J., Dekker, T. J., van de Horst, H. A., Eds.; Elsevier: Amsterdam, The Netherlands, 1987.

(11) te Velde, G.; Baerends, E. J. *J. Comput. Chem.* **1992**, *99*, 84.

Scheme 1. Fundamental Steps of the Polymerization Process

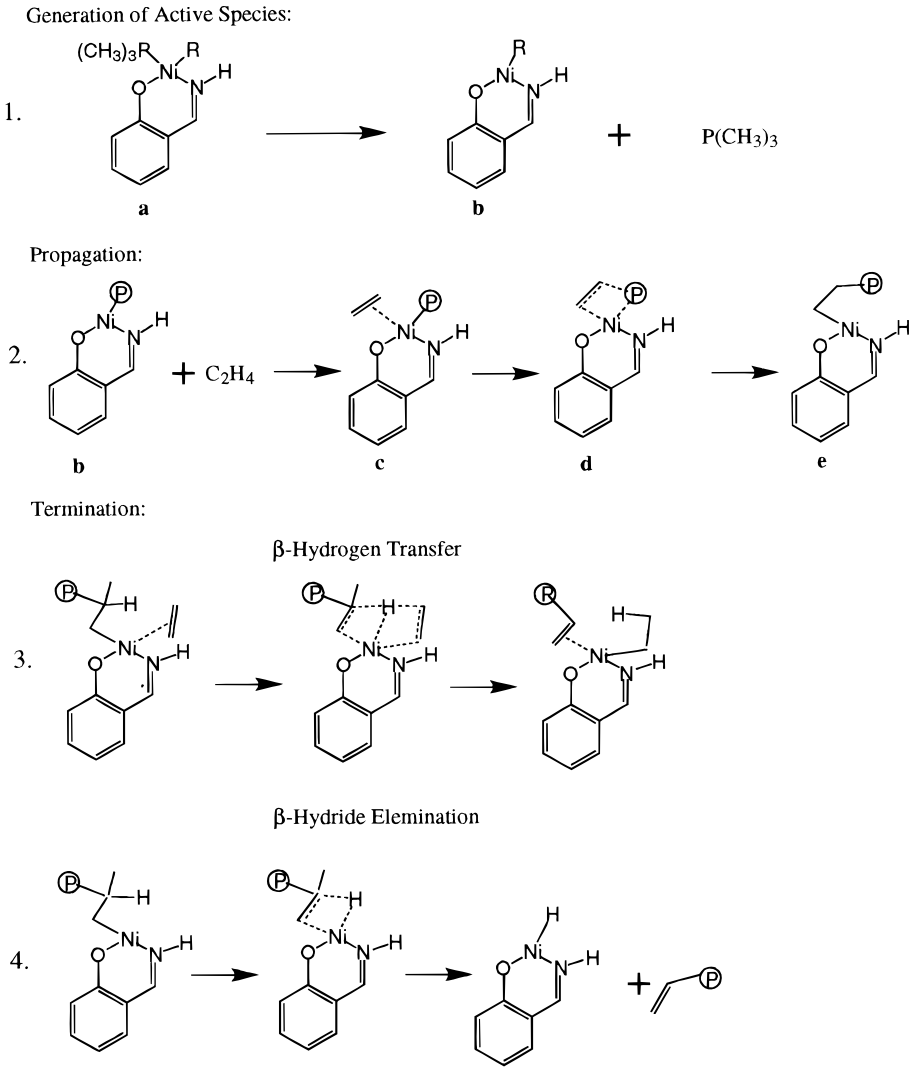

from Versluis and Ziegler.[12] Energy differences were calculated augmenting the local exchange−correlation potential by Vosko et al.[13] with Becke's nonlocal exchange corrections[14] and Perdew's nonlocal correlation corrections.[15] Geometries were optimized including these nonlocal corrections. The electronic configuration of Ni was treated with a Slater type triple-ζ basis function for the 4s and 3d orbitals, a double-ζ basis function on 3s and 3p orbitals, and single-ζ 4p polarization function. A double-ζ basis function for 3s and 3p as well as a single-ζ 3d polarization function was used to represent the valence orbital for P. The $1s^2$, $2s^2$, $2p^6$ on Ni and P was treated with the frozen core approximation. For the second-row elements N, C, and O, the $1s^2$ electronic configuration was treated with the frozen core approximation, a double-ζ basis function for 2s and 2p orbitals, and a single-ζ 3d polarization function. The hydrogen atom was represented by a double-ζ basis function for the 1s orbital and a single-ζ 2p polarization function. A set of auxiliary s, p, d, f, and g STO functions centered on all nuclei was used to fit the molecular density and represent Coulomb and exchange potentials accurately in each SCF cycle.[16] In view of the fact that all systems investigated in this work show a large HOMO−LUMO gap, a spin-restricted formalism was used for all calculations. The transition state geometries and energies were obtained by a series of geometry optimizations along a reaction coordinate. The value of the reaction coordinate was constrained, while all other parameters were optimized. The transition state was finally determined at the position where the gradient on this constraint was less than the threshold set for the optimization. The reaction coordinate used for the insertion reaction was the distance between the α carbon and one atom of the approaching ethylene (i.e., the C−C bond that is being formed). The reaction coordinate for termination reactions was the distance between the hydrogen atom being transferred and the *β*-carbon atom.

The combined DFT and molecular mechanics calculations were performed using the quantum mechanics/molecular mechanics (QM/MM) implementation into the ADF program.[17] It incorporates a modified Amber95[18] force field that includes Rappé's universal force field (UFF) van de Waals parameters for nickel.[19] All force field parameters are provided as Supporting Information. The partition scheme developed by Morokuma and Maseras was used to couple the QM and the MM regions. For system **4** the pure QM region consisted of the core

(12) Versluis, L.; Ziegler, T. *J. Chem. Phys.* **1988**, *88*, 322.
(13) Vosko, S. H.; Wilk, L.; Nusair, M. *Can. J. Phys.* **1980**, *58*, 1200.
(14) Becke, A. *Phys. Rev. A* **1988**, *38*, 3098.
(15) Perdew, J. *P. Phys. Rev. B* **1986**, *34*, 7406.
(16) Krijn, J.; Baerends, E. J. *Fit Functions in the HFS-Method*; Free University of Amsterdam, 1984.
(17) Woo, T. K.; Cavallo, L.; Ziegler, T. *Theor. Chim. Act.* **1998**, *100*, 307.
(18) Cornell, W. D.; Cieplk, P.; Bayly, C. I.; Gould, I. R.; Merz, K. M., Jr.; Ferguson, D. M.; Spellmeyer, D. C.; Fox, T.; Caldwell, J. W.; Koolman, P. A. *J. Am. Chem. Soc.* **1995**, *117*, 5179.
(19) Rappé, A. K.; Casewit, C. J.; Colwell, K. S.; Goddard, W. A., III; Skiff, W. M. *J. Am. Chem. Soc.* **1992**, *114*, 10024.

catalyst whose structure can be represented by system **3**. The pure MM region consists of the 2,6-diisopropylphenyl group. The coupling of the two regions occurs at the N(imine)−C(aryl) bond. In the theoretical model, two bond lengths are involved, the N(imine)−H bond in the pure QM region and the N(imine)−C(aryl) bond that crosses into the MM region. The two bonds are coupled such that the difference in their lengths, ΔR, is fixed throughout the calculation. For the imine connection, ΔR was set to 0.42 Å, giving an N(imine)−C(aryl) bond length of roughly 1.45 Å, close to the 1.434 Å obtained from full QM optimization. The partition scheme for system **5** is the same as that for system **4** with the addition of the anthracenyl group in the MM region. The ΔR for the C(aryl)−C(aryl) coupling was also set at 0.42 Å, giving a bond length of roughly 1.53 Å. The partition for system **6** is identical to the system **5**. For system **6**, the ΔR was also set to 0.42 Å for the P−C(aryl) bond, giving a bond length of roughly 1.85 Å, close to the 1.843 Å obtained from full QM optimization. In addition, the improper torsion around the phosphorus was constrained at 175.03° in all optimizations for system **6** to conform to the planar structure obtained from full QM studies. The enthalpy energy differences discussed throughout this study do not contain zero-point energy correction or finite temperature contributions. They can as such also be considered as potential energy differences.

III. Results and Discussion

a. Generation of the Active Catalyst. The generation of the active site in the salicylaldiminato nickel complexes is modeled by the phosphine dissociation energy as depicted by reaction 1 of Scheme 1. Several conformations for the catalyst precursor of the model system **1a** were examined. The lowest energy conformer found showed a square planar geometry around the nickel with the propyl chain trans to the oxygen. The conformation of the propyl chain extends straight out from the metal center, with the Ni−C_α−C_β−C_γ dihedral angle being 178.5°. The lowest energy conformer of the active catalyst after phosphine dissociation, **1b**, also has the propyl chain positioned trans to the oxygen. However, the chain in this structure is rotated toward the nickel so as to facilitate a β-agostic interaction between one hydrogen atom on the β-carbon and the metal, resulting in a Ni−C_α−C_β−C_γ dihedral angle of 116.0°. This serves to alleviate some of the electron deficiency of the metal center. The optimized structures of **1a** and **1b** can be found in Figure 3 with selected bond distances reported in units of angstroms. The structural features of catalyst precursor (**a**) and activated catalysts (**b**) are similar for the other five systems. Their structures are not reproduced but are included in the Supporting Information.

The enthalpy change (ΔH) with regard to the phosphine dissociation reaction for the six systems investigated is reported in Table 2. The results for systems **1**, **2**, and **3** clearly suggest that the electronic nature of the substituent on the 5 position of the salicylaldiminato ligand does not have strong influences on the phosphine dissociation enthalpy. The incorporation of an electron-donating methoxy group shows little effect on the reaction energy. The electron-withdrawing nitro group, as expected, increases the phosphine dissociation energy. However, the magnitude of the change is relatively small at 0.9 kcal/mol. The addition of a bulky 2,6-diisopropylphenyl group on the imine nitrogen in system **4** has little effect on the phosphine dissociation energy.

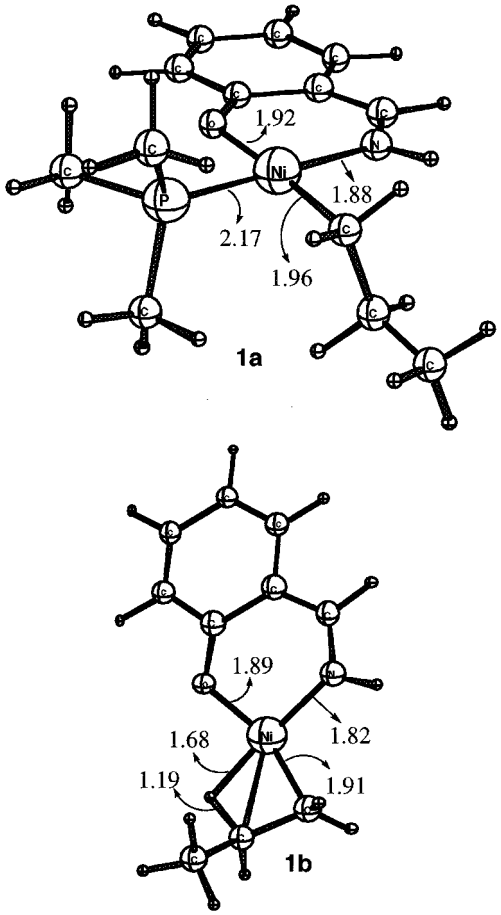

Figure 3. Optimized structure of the catalyst precursor and activated complex for catalyst system **1**.

Table 2. Enthalpy Change for the Phosphine Dissociation Reaction

catalyst system	ΔH (kcal/mol)
1	27.3
2	27.5
3	28.2
4	27.9
5	23.7
6	20.9

This can be explained by the observation that the phosphine ligand is trans to the aromatic substituent, and therefore, the steric bulk is expected to have little effect. System **5**, on the other hand, shows a marked decrease in phosphine dissociation energy due to the presence of the bulky anthracenyl group on the 3 position of the salicylaldiminato ligand. The difference of 3.7 kcal/mol between catalysts **4** and **5** can be attributed to the destabilization of the phosphine complex **5a** due to steric repulsion of the anthracenyl group and the phosphine ligand. The 2.8 kcal/mol difference in ΔH between systems **5** and **6** is due to the electronic effects of the donor atom. The higher electronegativity of the nitrogen atom relative to the phosphorus makes the imine catalyst less effective at stabilizing the electron-deficient nickel center in system **5**.

b. Chain Propagation. Chain propagation in the salicylaldiminato nickel complexes is assumed to follow the generally accepted Cossée−Arlman mechanism for insertion as shown by reaction 2 in Scheme 1.[20] The insertion is initiated by the complexation of the incoming olefin to the electron-deficient metal center in (**b**)

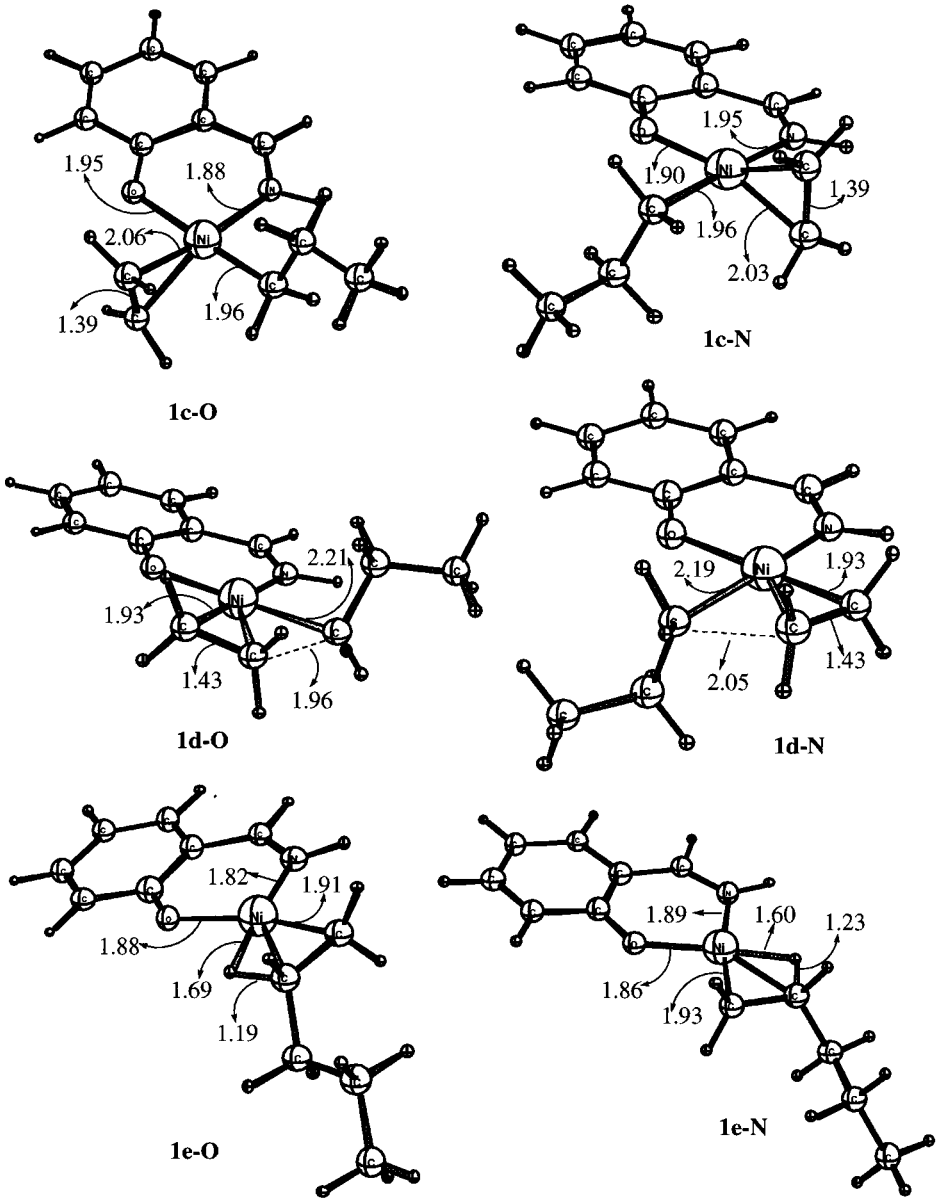

Figure 4. Optimized structures of complexes involved in the insertion process for catalyst system **1**.

to form a π-complex (**c**). This complexation assists the insertion of the olefin into the metal−carbon bond via a four-member cyclic transition state (**d**). The product of the insertion (**e**) resembles the starting material (**b**) in that a new vacant coordination site is available for the next olefin to coordinate and propagate the chain.

The optimized structures of the complexes for the model system **1** involved in the insertion process are shown in Figure 4. The bond distances in Figure 4 are reported in angstroms. Two geometrical isomers each are possible for the π-complex **1c**, the transition state **1d**, and the insertion product **1e**, one where the alkyl chain is located trans to the oxygen (denoted as **-O** in Figure 4) and the other where the alkyl chain is trans to the nitrogen (denoted as **-N**). The orientation of the ethylene in the π-complex is such that the double bond is oriented perpendicular to the plane formed by the aromatic ring of the catalyst. The two olefinic carbon atoms are both located at 2.05 Å from the nickel in both isomers of the π-complex. The ethylene remains planar, indicating a pure π-interaction at this stage. In the transition state, the olefin is rotated by 90° into the molecular plane of the catalyst to facilitate insertion into the metal−carbon bond. The formation of the new carbon−metal bond is complete at this stage, as indicated by the short Ni−C_α bond length of 1.93 Å. This is accompanied by the lengthening of the olefin double bond from 1.39 Å in the π-complex to 1.43 Å in the transition state and partial formation of the $C_{(propyl)}$−$C_{(olefin)}$ bond at an interatomic distance of 1.960 Å for **1d-O** and 2.052 Å for **1d-N**. The thermodynamic products from the insertion (**1e-O** and **1e-N**) exhibit β-agostic bonds, as evidenced by the long C−H bond distances of 1.23 and 1.19 Å, respectively. The geometries of the π-complex (**c**), insertion transition state (**d**), and insertion product (**e**) for the other systems studied are included in the Supporting Information.

The reaction profile for the insertion from both π-complex isomers can be found in Figure 5. The structure with the alkyl chain trans to the oxygen is

(20) (a) Cossée, P. *J. Catal.* **1964**, *3*, 80. (b) Arlman, E. J. *J. Catal.* **1964**, *3*, 89. (c) Arlman, E. J.; Cossée, P. *J. Catal.* **1964**, *3*, 99.

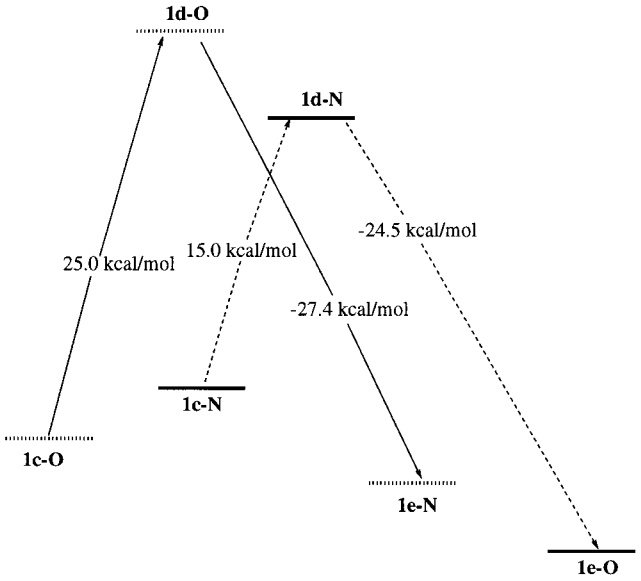

Figure 5. Reaction profile for the insertion of system **1**.

the more stable of the two isomers for the π-complex (**c**) and the insertion product (**e**). However, the transition state arising from **1c-N** is of lower energy than the one arising from the **1c-O** as a result of the trans-directing effect of the nitrogen atom. The destabilization of the π-complex and stabilization of the transition state make the insertion barrier from the **1c-N** isomer much lower than from **1c-O**. It is worthwhile to note that the insertion from the ethylene complex with the alkyl trans to the oxygen results in a resting state with the alkyl trans to the nitrogen. This indicates that the two pathways would alternate as the polymerization proceeds. In light of the large barrier of 25.0 kcal/mol encountered for the ethylene complex **1c-O**, isomerization to **1c-N** may occur before insertion. The barrier to isomerization for the ethylene complexes (**1c-O** to **1c-N**) as well as from the active species (**1b-O** to **1b-N**) was studied. The latter can also be considered as isomerization at the resting state. The barrier to isomerization was 11.4 kcal/mol from the ethylene complex and 36.6 kcal/mol from the active species. The relative energy of these barriers suggest that isomerization occurs at the olefin complex stage and isomerization to **1c-N** is more favorable than insertion. The most energetically favorable pathway for insertion is summarized in Scheme 2. The more stable active catalyst, **1b-O**, would be present in higher concentration. The reaction of this complex with one molecule of ethylene occurs in step 1 to produce the more stable olefin π-complex **1c-O**. Since the barrier to insertion is high, this π-complex undergoes cis−trans isomerization to **1c-N,** as shown in step 2. In the final step, olefin insertion occurs from **1c-N** to produce **1e-O** through the more stable transition state **1d-N**. Note that **1e-O** is equivalent to **1b-O** with an additional monomer unit and therefore can propagate the polymer chain by cycling through the same three steps.

The ethylene complexation energy and the insertion barrier for the six systems studied are reported in Table 3. The complexation enthalpy is calculated as the energy difference between the appropriate π-complex (**c**) and the sum of the activated complex (**b**) plus an isolated ethylene molecule. The insertion barrier is obtained from the energy difference between the π-complex (**c**) and the insertion transition state (**d**). Note that the geometrical arrangement around the nickel has a large effect on the insertion barrier. Comparing the results for catalyst systems **1**, **2**, and **3**, we see that the electronic nature of the substituent at the 5 position of the salicylaldiminato ligand produces a very minor effect on the energetics of the insertion process. The electron-releasing methoxy group increases the barrier slightly, while the electron-withdrawing nitro group decreases the insertion barrier by 1.5 kcal/mol. The small energy differences between system **3** and system **4** indicate that the diisopropylphenyl group also has little influence on the olefin insertion process. The lack of changes in the olefin complexation energy is a result of the bulky group being trans to the incoming olefin, where it is too far for steric effects to have any influence. The small effect on the insertion barrier can also be rationalized by steric considerations. In the insertion transition state of system **4**, the phenyl ring of the diisopropylphenyl group is almost perpendicular (at 87°) to the plane formed by the aromatic rings of the catalyst. In this conformation, most of the steric bulk of the isopropyl groups is located above and below this plane. For this reason, the added functional group is not expected to have a large effect on the insertion transition state structure or its energy because the olefin is forced to take up an equatorial position around the metal center to facilitate the formation of the new C−C bond. The results from systems **4** and **5** provide an indication of how the anthracenyl group affects the energetics of insertion. A dramatic decrease of 6.0 kcal/mol is observed in the ethylene complexation energy. This is due to the steric repulsion between the olefin and the anthracenyl group as it approaches the metal. Despite such destabilization of the π-complex, this functional group lowers the actual insertion barrier only by 1.0 kcal/mol. Finally, the differences between systems **5** and **6** show the influence of substituting the nitrogen donor atom with a phosphorus atom. The complexation energy is decreased slightly by this less electronegative phosphorus, but the insertion barrier is raised by almost 1.6 kcal/mol.

c. Termination. Two possible chain termination pathways were initially explored for system **4**. This catalyst system was chosen because it contained structural features that would show electronic as well as steric effects. Figure 6compares the reaction profile for the β-hydrogen transfer (BHT) reaction (Scheme 1, reaction 3) and β-hydrogen elimination (BHE) (Scheme 1, reaction 4) mechanisms of termination. The optimized structures of the complexes in this reaction profile can be found in Figures 7 and 8 for the BHE and BHT mechanisms, respectively. Selected bond distances are included in units of angstroms. The transition state for BHE reaction (**4f**) lies 12.5 kcal/mol above the active catalyst (**4b**). Just 0.6 kcal/mol below the transition state lies the structure of a nickel hydride with a propylene attached in the coordination sphere (**4g**). Further investigations show that dissociation of the propylene molecule from **4g** is endothermic by 38.0 kcal/mol. In light of this, the BHT mechanism is still the preferred pathway even though the BHT transition state lies 1.3 kcal/mol higher in energy than the BHE

Scheme 2. Lowest Energy Insertion Pathway for Catalyst System 1

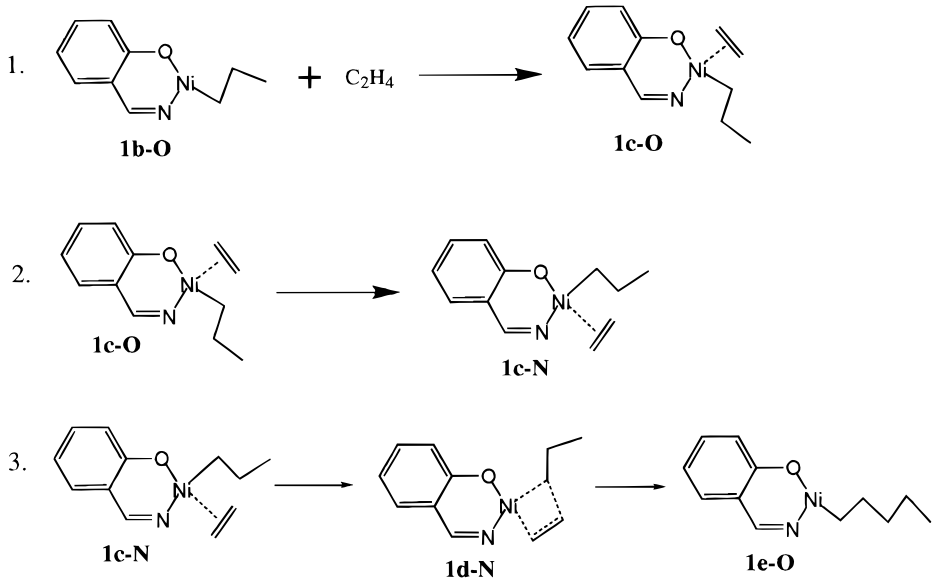

Table 3. Calculated Olefin Complexation and Insertion Barriers from Two Isomers

	olefin complexation energy (kcal/mol)		insertion barrier (kcal/mol)	
catalyst	alkyl trans to N	alkyl trans to O	alkyl trans to N	alkyl trans to O
1	−18.2	−17.1	15.3	25.0
2	−18.3	−17.4	15.5	25.0
3	−17.1	−16.7	14.1	24.0
4	−16.1	−16.1	14.0	24.3
5	−17.1	−11.1	14.0	23.3
6	−16.8	−10.8	15.6	26.0

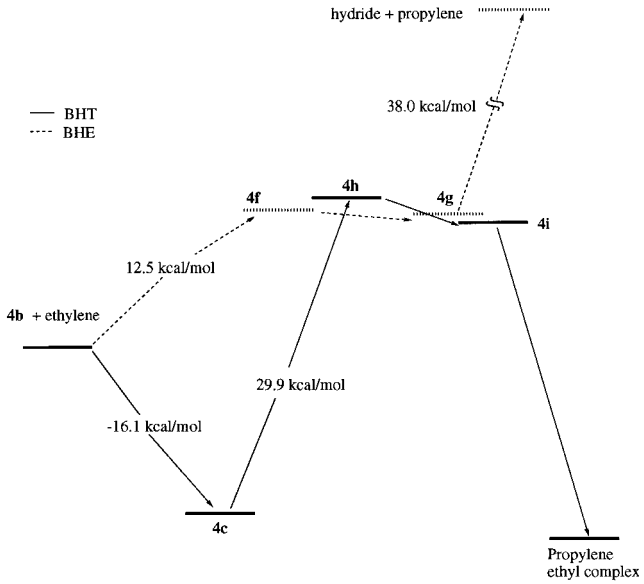

Figure 6. Reaction profile for the termination of catalyst system **4**.

transition state on the relative energy profile. Therefore, only the BHT mechanism was considered for the other systems.

The BHT reaction begins from the olefin π-complex (**4c**). The BHT transition state from both isomers of were searched for; however, only the one from **4c-O** converged. This transition state (**4h**) lies 29.9 kcal/mol above the olefin π-complex. Proceeding past the transition state, the energy drops slightly by 2.6 kcal/mol into a shallow minimum that can be describe as a nickel hydride coordinated with two olefins (**4i**). Previous studies on the Brookhart catalyst found that this metal hydride proceeded to form a stable propylene complex with an ethyl chain that is just slightly more stable than the starting ethylene π-complex.[2f] Similar behavior can be expected from the system presently under investigation. Optimization of the transition state from **4c-N** resulted in dissociation of the ethylene from the nickel center. However, the BHT transition states from both π-complex isomers were obtained for system **3**. Unlike the insertion barriers, there is little difference between the termination barriers from either isomer. The transition state from **3c-O** lies 23.9 kcal/mol above the π-complex, while the barrier from **3c-N** is 23.7 kcal/mol. Due to the small difference between these two barriers, only the transition state from the more stable **-O** isomer was explored for the other systems. The energy and geometry of the BHT transition state (**h**) and the diolefin complex (**i**) for the other systems are included in the Supporting Information.

The termination barrier via the BHT mechanism is 25.7, 26.2, and 23.9 kcal/mol for systems **1**, **2**, and **3**, respectively. This shows that the electronic nature of the substituent at the 5 position also does not have a large effect on the termination barrier. The electron-releasing methoxy group tends to increase the barrier by destabilizing the transition state, while the electron-withdrawing nitro group decreases the barrier with a stabilizing effect. The addition of the bulky diisopropylphenyl group on the catalyst increases the termination barrier by 6.0 kcal/mol, as shown by the barrier of 29.9 kcal/mol for system **4**. This large influence on the stability of the termination transition state has been observed experimentally and rationalized theoretically with the Brookhart diimine catalyst.[2b,d,e] The increased barrier is due to the destabilization of the transition state by steric repulsion between the bulky aryl group and ligands that are forced to take up an axial position. Interestingly, the addition of a second bulky aryl group, the 9-anthrancenyl group on the 3 position, did not further increase the termination barrier. The transition

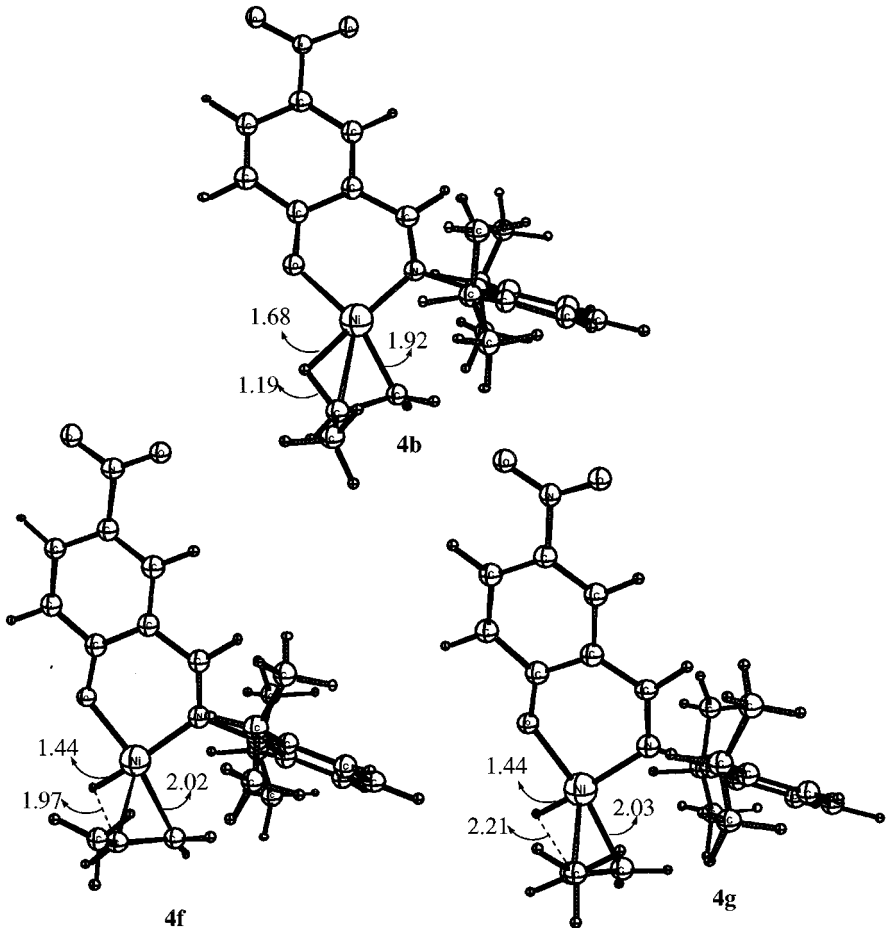

Figure 7. Optimized structures for the complexes involved in the BHE termination of catalyst system **4**.

state for system **5** lies 29.3 kcal/mol above the olefin π-complex, indicating that the 9-anthrancenyl group has little effect on the termination barrier. Finally, replacing the nitrogen donor atom with phosphorus lowers the termination barrier to 26.0 kcal/mol for system **6**. A comparison of the geometries of the transition states for systems 5 and 6 showed that the major difference is caused by the different lengths of the Ni−N and Ni−P bonds. The longer Ni−P and P−C bonds (2.24 and 1.86 Å, respectively) compared to the Ni−N and N−C bonds (1.97 and 1.45 Å, respectively) move the bulky diisopropylphenyl group further away from the reaction center and thus reduce the steric repulsion encountered by the alkyl ligands.

d. Influence of Substituents on Catalyst Activity. A comparison of the reaction enthalpies and barriers obtained for systems **1**, **2**, and **3** shows that the electronic nature of the substituent at the 3 position has the least influence on the energetics of all the fundamental steps in the polymerization process. Even so, electron-withdrawing groups tend to vary the energies in favor of polymerization, as it decreases the phosphine dissociation energy and the insertion barrier while only lowering the termination barrier slightly. Electron-releasing groups tend to alter the energetics in the direction that would hinder polymerization by increasing the phosphine dissociation energy and insertion barrier while decreasing the termination barrier. The changes caused by the variation at this position are relatively small. The largest difference was found to be 1.8 kcal/mol for the termination barrier. Therefore, substitution at this position is not expected to have dramatic effects on the catalyst activity. The small changes observed are likely due to the remoteness of this substituent from the reaction center. The large distance diminishes the electronic effects felt by the active nickel center. Varying the electronic nature of the donor atom(s) results in larger changes in the energies, as can be seen by replacing the nitrogen adjacent to the nickel with a phosphorus (systems **5** and **6**). This variation in the catalyst composition decreases the phosphine dissociation energy as the less electronegative phosphorus increases the electron density on the metal center. This would serve to enhance catalyst activity. However, system **6** has a lower termination barrier, which would hinder its ability to act as an efficient catalyst. Consequently, the effect of this structural modification on the catalyst activity is not easily predictable due to the opposing trends observed.

The dominant effect of adding the 2,6-diisopropylphenyl group to the imino ligand is to increase the termination barrier by 6.0 kcal/mol. This is caused by the destabilization of the transition state due to steric repulsion between the aryl group and alkyl ligand undergoing the reaction. The function of the 9-anthracenyl group on the 3 position is to decrease the phosphine dissociation energy by 4.2 kcal/mol. This is also a steric effect where the catalyst precursor is destabilized by the steric repulsion between this substituent and the phosphine ligand. The results obtained by system **3**, **4**, and **5** clearly show that the addition of bulky substituents to either side of the catalyst should

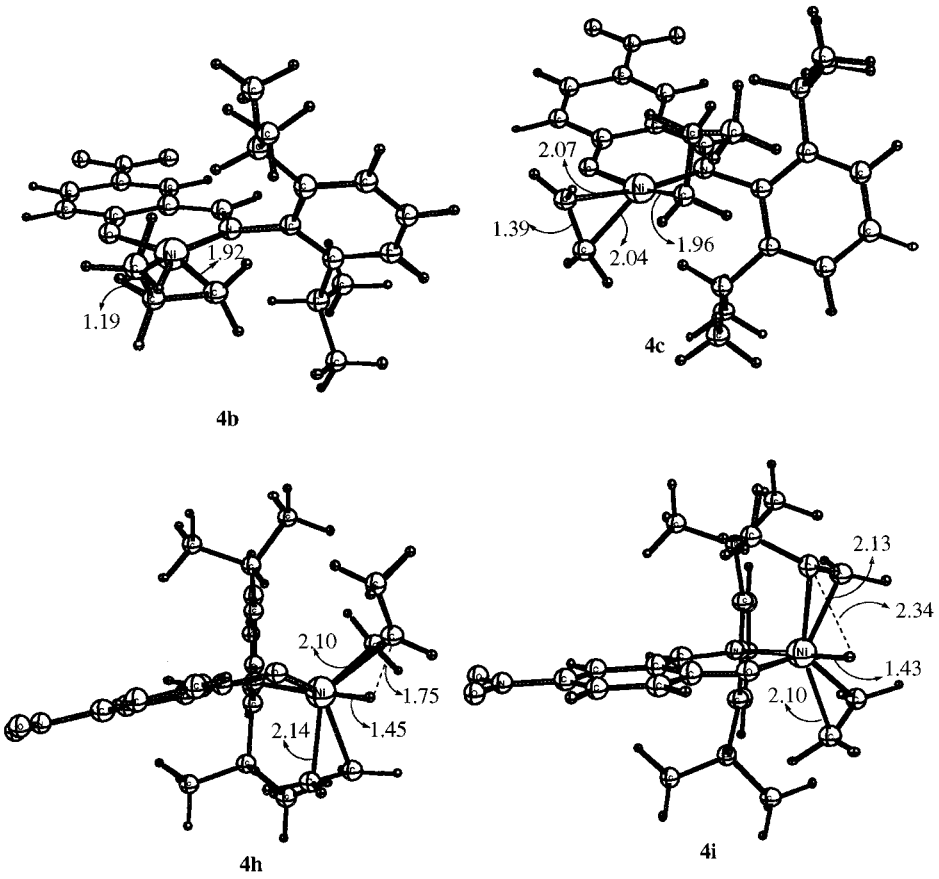

Figure 8. Optimized structures for the complexes involved in the BHT termination of catalyst system **4**.

enhance catalytic activity. In addition, the changes caused by steric factors are significantly larger than those due to electronic factors.

e. Comparison with Experimental Observations. The trends in the phosphine dissociation energy reported in Table 2 for the six systems studied in this investigation indicated that the bulky R group on the 3 position of the salicylaldiminato ring is the only substitution that causes a significant change in the enthalpy of this activation step. The addition of this group lowers the dissociation energy by 4.5 kcal/mol. On the other hand, the insertion barrier was found to be relatively insensitive to changes in the catalyst backbone, as illustrated in Table 3. The above observations lend support to the hypothesis that the induction period observed is a result of slow dissociation of the phosphine ligand from the nickel complex rather than slow insertion, as has been suggested from analogy with the SHOP systems.[21]

The increase in catalyst activity of adding bulky substituents on the salicylaldiminato ring predicted by the present DFT studies agrees well with the experimental observation that these groups enhance the activity by a factor of 3. The trends obtained from studying the electronic factors also agree with the experimental observations in that electron-withdrawing groups on the catalyst backbone enhance catalyst activity while electron-releasing groups hinder catalyst activity. However, the small changes in energy obtained from the DFT calculations is not compatible with the large enhanced activity observed experimentally due to the addition of a nitro group on the para position. A recent study on the electronic effects of meta and para substituents on the vanadium center of O,N-chelated vanadium(IV) oxophenolate complexes found linear relationships between the Hammett constant σ and UV−vis absorption, EPR, and redox behavior of these complexes.[22] This suggests a linear response to changes in the electronic nature of the substituents, in agreement with the calculated results and in contrast to the large jumps in activity observed experimentally. Further support for the small electronic effect of the substituents is that for UV−vis absorption and EPR the slopes were relatively small compared with the magnitude of the properties themselves. In light of the small changes obtained from electronic factors, the 10-fold increase in catalyst activity observed by Grubbs cannot be completely attributed to electronic factors.

IV. Conclusions

The results of the present density functional study on the six salicylaldiminato nickel complexes as potential olefin polymerization catalysts indicate that these complexes can be activated by the dissociation of the phosphine group. The insertion is initiated by the complexation of a monomer to the activated complex. There are significant differences in the barrier to insertion depending on the geometrical isomer of the

(21) (a) Klabunde, U.; Ittel, S. D. *J. Mol. Catal.* **1987**, *41*, 123. (b) Klabunde, U.; Mulhaupt, R.; Herskovitz, T.; Janowicz, A. H.; Calcbrese, J.; Ittel, S. D. *J. Polym. Sci. Part A: Polym. Chem.* **1987**, *25*, 1989.

(22) Hagen, H.; Barbon, A.; van Faassen, E. E.; Lutz, B. T. G.; Boersma, J.; Spek, A. L.; van Koten, G. *Inorg. Chem.* **1999**, *38*, 4079.

olefin π-complex. Insertion from the isomer with the alkyl chain trans to the nitrogen is the more favorable pathway. Since the insertion of an ethylene unit changes the configuration of the chain with respect to the salicylaldiminato ligand, isomerization occurs at the π-complex stage so that insertion could proceed through the lower energy transition state. The β-hydrogen transfer mechanism for the termination was found to be energetically more favorable than the β-hydrogen elimination mechanism. The termination barriers found were generally higher than the insertion barriers. Therefore, these neutral salicylaldiminato nickel complexes have the potential to be polymerization catalysts and their activity can be refined by variations in the structure of the catalyst backbone.

A comparison of the results obtained by varying the substituents on the catalyst backbone led to the conclusion that the electronic nature of the substituent at the 5 position of the salicylaldiminato ligand should have little effect on the catalyst activity. On the other hand, changing the electronic nature of the donor atoms has a moderate effect on the energies of the polymerization reactions. However, its influence on catalyst activity cannot be easily predicted due to the opposing trends observed. Finally, the addition of bulky substituents on the catalyst backbone should enhance catalyst activity.

Acknowledgment. This investigation was supported by the Natural Science and Engineering Research Council of Canada (NSERC) and by Novacor Research and Technology (NRTC) of Calgary, Alberta, Canada. We wish to thank Dr. Artur Michalak for helpful discussions.

Supporting Information Available: Table of force field parameters used for the QM/MM calculations as well as tables of gas-phase energies and Cartesian coordinates of DFT optimized structures of **a**−**e** and **h**,**i** for all six catalyst systems and **f**,**g** for systems **3** and **4**. This material is available free of charge via the Internet at http://pubs.acs.org.

OM000055+